Trebuchet Sling Length and Projectile Range

Candidate Personal code: lsm430
Word Count: 3000 Words

May 2025

1 Research Design

1.1 Introduction

The range achieved by a medieval trebuchet was critical in sieges; exploring how sling length affects this distance offers potential insights into optimizing its design. Intrigued by this historical application of physics, I chose to investigate how varying only the sling length impacts the horizontal range and release angle of a model trebuchet's payload. To isolate this variable's effect, key parameters such as counterweight mass, lever arm dimensions, drop height, and fulcrum position were kept constant throughout the experiment. While trebuchet mechanics bridge classical physics and engineering applications, understanding the specific relationship between sling length, range, and release angle is essential for evaluating performance and appreciating the underlying mechanics of this historical technology.

1.2 Research Question

"How does varying the sling length (0.10, 0.15, 0.20, 0.25, 0.30, 0.35, 0.40 m) of a trebuchet affect the horizontal range and release angle of the payload when the height, lever arm length, and position of the fulcrum are kept constant?"

1.3 Background Information

The horizontal range of a trebuchet's payload is a key measure of its performance, determined by the physics of projectile motion after release from the sling, while the release angle defines the trajectory's initial direction. This investigation focuses on how the sling length (L_s) affects both this range (R) and the release angle (θ), with the height, lever arm length, and fulcrum position held constant. To understand this relationship, we start with the standard range equation for a projectile launched from ground level, as derived in fundamental physics:

$$R = \frac{v_0^2 \sin(2\theta)}{g} \tag{1}$$

Where:

- R = horizontal range (m),
- v_0 = initial velocity of the payload at release (m/s),
- θ = release angle relative to the horizontal (°),
- g = gravitational acceleration (9.81 m/s^2).

This equation assumes the payload follows a parabolic trajectory after leaving the sling, with R maximized when $\theta = 45°$, as $\sin(2\theta) = 1$. In a trebuchet, both v_0 and θ are influenced by the sling length (L_s), requiring further derivation to connect R and θ to L_s.

The trebuchet operates by converting the gravitational potential energy of a counterweight into the kinetic energy of the payload. Consider the counterweight (mass m_c) falling a fixed height (h):

$$PE = m_c g h \tag{2}$$

Where:

- PE = potential energy (J),
- m_c = counterweight mass (kg, constant),
- h = drop height (m, constant).

This energy is transferred to the payload (mass m_p) at release, becoming its kinetic energy:

$$KE = \frac{1}{2} m_p v_0^2 \tag{3}$$

Where:

- KE = kinetic energy (J),
- m_p = payload mass (kg, constant).

Assuming ideal energy transfer (neglecting friction and air resistance for simplicity):

$$PE = KE \tag{4}$$

Substitute equations (2) and (3):

$$m_c g h = \frac{1}{2} m_p v_0^2 \tag{5}$$

Solve for v_0^2 by isolating it:

$$v_0^2 = \frac{2 m_c g h}{m_p} \tag{6}$$

This suggests v_0^2 is constant if m_c, h, and m_p are fixed. However, the trebuchet's lever arm and sling amplify the payload's velocity through rotational motion. The payload's release velocity is the tangential velocity at the sling's end, determined by the angular velocity (ω) of the system and the distance from the fulcrum to the payload:

$$v_0 = \omega (L_a + L_s) \tag{7}$$

Where:

- ω = angular velocity of the lever arm (rad/s),
- L_a = lever arm length from fulcrum to sling attachment (m, constant),
- L_s = sling length (m, varied: 0.10, 0.15, 0.20, 0.25, 0.30, 0.35, 0.40 m).

Square this to align with the range equation:

$$v_0^2 = \omega^2 (L_a + L_s)^2 \tag{8}$$

Revisit energy conservation using this velocity:

$$m_c g h = \frac{1}{2} m_p [\omega (L_a + L_s)]^2 \tag{9}$$

Simplify:

$$m_c g h = \frac{1}{2} m_p \omega^2 (L_a + L_s)^2 \tag{10}$$

Solve for ω^2:

$$\omega^2 (L_a + L_s)^2 = \frac{2 m_c g h}{m_p} \tag{11}$$

$$\omega^2 = \frac{2 m_c g h}{m_p (L_a + L_s)^2} \tag{12}$$

Substitute back into (8):

$$v_0^2 = \left(\frac{2 m_c g h}{m_p (L_a + L_s)^2} \right) (L_a + L_s)^2 \tag{13}$$

$$v_0^2 = \frac{2 m_c g h}{m_p} \tag{14}$$

This matches equation (6), confirming consistency in an idealized model. However, in reality, ω and θ adjust with L_s due to the sling's effect on release timing. Literature (e.g., [1, 2]) suggests longer L_s increases the acceleration arc but delays release, altering θ. For simplicity, assume v_0 scales with $L_a + L_s$ via a constant k (incorporating ω effects):

$$v_0 = k (L_a + L_s) \tag{15}$$

Where:

- k = a proportionality constant (1/s). Note: The units here should be 1/s if v0 has units m/s and (La+Ls) has units m. k represents an effective angular velocity factor.

Square it:

$$v_0^2 = k^2 (L_a + L_s)^2 \tag{16}$$

Substitute into (1):

$$R = \frac{k^2 (L_a + L_s)^2 \sin(2\theta)}{g} \tag{17}$$

This final equation represents the theoretical relationship between the sling length and the horizontal range of the trebuchet's payload, with θ as a critical factor. It shows that the range (R) increases quadratically with the combined length of the lever arm and sling ($L_a + L_s$), scaled by a proportionality constant (k) that accounts for the system's

rotational dynamics. The term $\sin(2\theta)$ reflects the dependence on the release angle, which varies with L_s due to the sling's influence on the timing and position of release. The gravitational acceleration (g) in the denominator indicates that R is inversely proportional to the strength of gravity, consistent with projectile motion principles. This formula assumes idealized conditions (e.g., no energy losses), and experimental data will test its predictions by measuring both R and θ for different L_s values.

The variables in this formula are defined as follows:

- R: Horizontal range of the payload (m), the distance from the release point to the landing point.
- k: Proportionality constant (1/s), encapsulating the effects of angular velocity and energy transfer efficiency.
- L_a: Lever arm length (m), the fixed distance from the fulcrum to the sling attachment point (0.4133 m in this study).
- L_s: Sling length (m), the variable distance from the lever arm attachment to the payload pouch (varied: 0.10, 0.15, 0.20, 0.25, 0.30, 0.35, 0.40 m).
- θ: Release angle (°), the angle of the payload's initial velocity relative to the horizontal at the moment of release, influenced by L_s.
- g: Gravitational acceleration (m/s^2), taken as 9.81 m/s^2 in this experiment, acting as a constant.

Since L_a is constant, R depends on L_s and θ, with θ varying with L_s due to release dynamics (measured experimentally). This is the theoretical relationship for this investigation.

To visualize the forces, consider **Figure 1** (self-designed using drawing software): a free-body diagram of the payload in the sling during rotation. The forces include:

- **Tension (T)**: Along the sling toward the lever arm, providing centripetal force.
- **Gravitational force ($F_g = m_p g$)**: Downward, contributing to motion.
- At release, tension drops, and v_0 (tangential) and θ define the trajectory.

This derivation and diagram show R increases quadratically with $L_s + L_a$, modulated by θ, aligning with trebuchet mechanics.

1.4 Hypothesis

It is hypothesized that the collected data and subsequent analysis will reveal a non-linear relationship between the sling length (L_s) and both the horizontal range (R) and release angle (θ), with an optimal L_s maximizing R and corresponding to a specific θ. This hypothesis is supported by the principles of projectile motion and trebuchet mechanics outlined in the Background Information section. According to the derived formula:

$$R = \frac{k^2 (L_s + L_a)^2 \sin(2\theta)}{g} \tag{18}$$

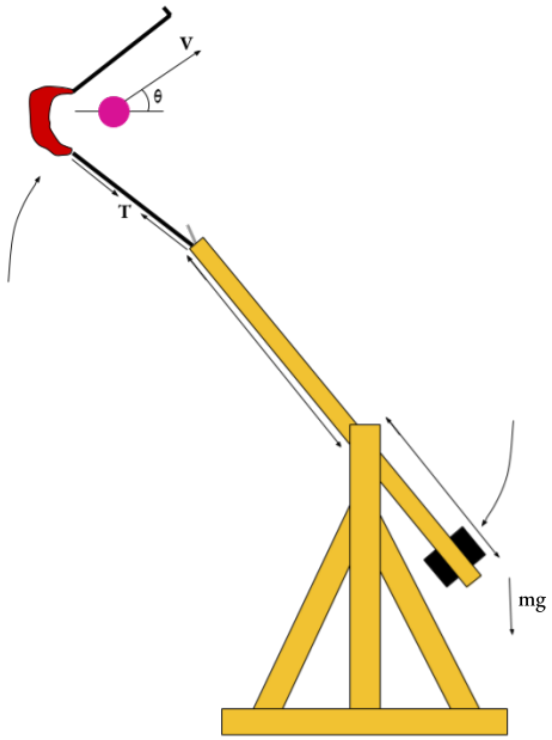

Figure 1: Free body diagram of trebuchet in action (self-designed using Google Drawings)

where L_a is the constant lever arm length (0.4133 m), g is the gravitational acceleration (9.81 m/s^2), and k is a proportionality constant (1/s), the range R depends on both the quadratic term $(L_s + L_a)^2$ and the release angle θ, which varies with L_s. As L_s increases from 0.10 m to 0.40 m, the term $(L_s + L_a)^2$ grows quadratically, potentially increasing the release velocity ($v_0 = k(L_s + L_a)$). However, literature suggests longer L_s delays release, reducing θ and thus $\sin(2\theta)$, while shorter L_s increases θ but reduces v_0 [1, 2]. An optimal L_s, potentially near the lever arm length L_a based on some theoretical models or optimized designs [2], balances these factors for maximum R (e.g., at $L_s \approx L_a = 0.4133$ m), with θ approaching 45° for maximum $\sin(2\theta)$. I hypothesize the graph of R versus L_s will resemble a parabola, peaking at this optimum (Figure 2), while θ versus L_s will decrease non-linearly as L_s increases (Figure 3).

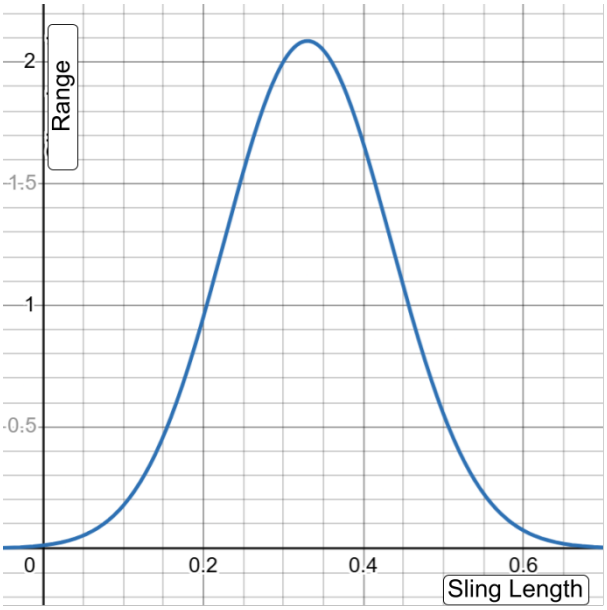

Figure 2: Hypothetical relationship between sling length and range (self-made using Desmos).

1.5 Variables

Variables	**Name**	**Explanation**	**Apparatus**
Independent variable	Sling length (L_s)	0.10, 0.15, 0.20, 0.25, 0.30, 0.35, 0.40 m. Varied by adjusting the sling's length between the lever arm attachment and payload pouch.	Ruler ($\pm$0.001 m)
Dependent variable	Horizontal range (R)	Measured as the distance from the trebuchet's release point to the payload's landing point, determined by video analysis plotting horizontal displacement.	Commercial Measurement Tape ($\pm$0.005 m)
Dependent variable	Release angle (θ)	Measured as the angle of the payload's initial velocity relative to the horizontal at release, determined by video analysis tracking the sling's motion.	Camera, Tracker software ($\pm$0.5°)

Table 1: Independent and dependent variables with measurement uncertainties.

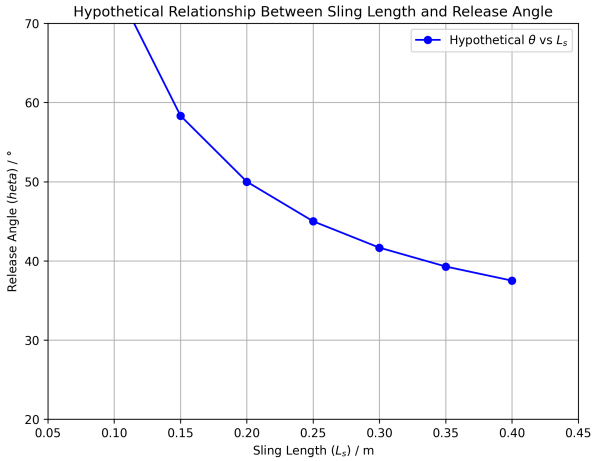

Figure 3: Hypothetical relationship between sling length and release angle (self-made using Desmos).

Variable	**Significance**	**Means of Control**
Lever arm length (L_a)	Affects the radius of rotation and release velocity (v_0). Must be constant to isolate L_s's effect on R and θ.	Fixed at 0.4133 m, measured with a ruler ($\pm$0.001 m).
Counterweight mass (m_c)	Influences potential energy and thus v_0. Variations could alter R and θ independently of L_s.	Set at 1.00 kg, measured with a digital scale ($\pm$0.001 kg).
Payload mass (m_p)	Impacts kinetic energy and trajectory. Must remain constant to focus on L_s.	Set at 0.050 kg (e.g., a small rubber ball), measured with a digital scale ($\pm$0.001 kg).
Drop height (h)	Determines potential energy input. Changes could affect v_0, R, and θ.	Fixed at 0.30 m, measured from counterweight's initial position with a measuring tape ($\pm$0.005 m).
Fulcrum position	Alters the lever arm's pivot point, affecting rotational dynamics. Must be fixed for consistency.	Secured at a constant position, 0.2067 m from the short arm end, verified with ruler ($\pm$0.001 m).
Gravitational acceleration (g)	Affects both energy transfer and projectile motion. Varies slightly by location.	Conducted at one location, assumed $g = 9.81$ m/s^2.
Environmental conditions	Wind or air resistance could influence R and θ.	Conducted indoors with minimal airflow, temperature measured at 20.0 $\pm$ 0.5°C (thermometer).

Table 2: Controlled variables with measurement uncertainties.

Variable	Significance
Air resistance	May slightly reduce R and alter θ, depending on payload shape and speed. Assumed minimal indoors, but potentially non-negligible for a light payload.
Friction at fulcrum	Could dissipate energy, reducing v_0, R, and θ. Assumed small with a smooth pivot, but likely present.
Sling elasticity	The wool cord may stretch slightly during launch, storing and releasing energy unpredictably, affecting v_0 and θ.

Table 3: Uncontrolled variables.

1.6 Materials

1. Trebuchet main arm made of Teakwood, length 0.62 m.
2. Trebuchet frame and supports made of Acacia Nilotica wood, dimensions approximately 0.3 m (height) $\times$ 0.60 m (base length).
3. Sling with adjustable length (0.10, 0.15, 0.20, 0.25, 0.30, 0.35, 0.40 m), made of wool cord and a cotton pouch.
4. Counterweight of 1.00 kg (metal weight).
5. Payload of 0.050 kg (small rubber ball).
6. Ruler ($\pm$0.001 m).
7. Digital scale ($\pm$0.001 kg).
8. Measuring tape ($\pm$0.005 m).
9. Camera
10. Tripod for camera stability.
11. Video analysis software "Tracker".
12. Thermometer ($\pm$0.5 °C).
13. Safety glasses.
14. Clear floor space (approx. 10 m x 3 m).

1.7 Methodology

1.7.1 Making the Trebuchet

1. Construct the Acacia Nilotica wood frame (approx. 0.3 m height $\times$ 0.60 m base length). Secure joints with screws to ensure stability and minimize wobbling during operation.
2. Attach the 0.62 m Teakwood main arm. Position the fulcrum 0.2067 m from the short arm end using a smooth pivot (e.g., metal axle) for free rotation; verify alignment with a ruler.

3. Affix the 1.00 kg counterweight to the short arm end, ensuring it hangs freely and achieves a 0.30 m drop height (measured with measuring tape).

4. Prepare an adjustable sling (wool cord, cotton pouch). Set initial sling length (L_s) to 0.10 m, measured from the long arm end to pouch center (ruler), and secure firmly.

5. Test structural integrity by manually rotating the weighted arm, checking for excessive flexing or misalignment before operation.

1.7.2 Operation of the Trebuchet

6. Verify counterweight (1.00 kg) and payload (0.050 kg) masses using a digital scale for consistency.

7. Set the counterweight drop height to 0.30 m (using measuring tape) from its lowest position, ensuring the long arm starts horizontally.

8. Position a camera on a tripod approx. 2.0 m away, perpendicular to the launch plane, centered on the trajectory. Ensure adequate background contrast for Tracker.

9. Maintain room temperature near 20.0°C (measured with thermometer) with minimal airflow; record temperature.

10. Don safety glasses. Clear the launch area of personnel and obstacles for at least 10 m.

11. Load the payload (0.050 kg), set the counterweight to its 0.30 m drop height, ensure the arm is correctly positioned, and start recording.

12. Release the counterweight smoothly and consistently to launch the payload. Stop recording after the payload lands and stops.

13. Mark the first landing point. Measure horizontal range (R) from the point vertically below release to the landing spot using a measuring tape; record R.

14. Upload video to Tracker software. Calibrate scale using a known length (e.g., 0.62 m arm). Track payload motion frame-by-frame post-release. Determine release angle (θ) from the velocity vector's angle to the horizontal immediately after release; record θ.

15. Repeat steps 6–9 four more times for the current L_s (total 5 trials), maintaining identical starting conditions.

16. Adjust L_s to the next value (0.15, 0.20, 0.25, 0.30, 0.35, 0.40 m) using the ruler, reattach securely, and repeat steps 6–10 for each L_s (35 total launches).

Figure 4: Experimental setup showing trebuchet, camera position, and measurement area (self-designed and constructed).

1.8 Preliminary Trials

Preliminary trials were conducted to optimize conditions and address challenges using the standard apparatus ($L_s = 0.20$ m, 1.00 kg counterweight, 0.05 kg payload). Initial range (R) inconsistency (6.5-7.2 m) was traced to sling pouch tangling affecting the release angle (θ). Adopting a smoother cotton pouch stabilized both R and θ measurements. Drop height testing confirmed that 0.3 m provided consistent launches with significant range and clearance, unlike 0.2 m; this validated the chosen height. Minor fulcrum wobbling slightly reduced R, necessitating firmer securing with screws. These refinements ensured subsequent variation of L_s (0.10 m to 0.40 m) would isolate its effects on R and θ. A baseline test ($L_s = 0.20$ m, Trial 1) yielding $R = 6.87$ m and $\theta = 14.4°$ validated the final setup.

1.9 Risk Assessment

Risk	Hazard Description	Mitigation Strategy
Projectile Injury	Payload (0.05 kg) launched at speed (potentially ¿10 m/s) could cause eye or impact injury if it strikes a person.	Experiment conducted in a designated, clear area (min. 10m length). A safety perimeter of at least 3 meters radius maintained around the trebuchet sides and back during operation. Ensure no individuals are within the launch path or perimeter during launches. Direction of launch is controlled and aimed away from people and fragile objects.
Trebuchet Structure Failure	Wooden components (Teakwood arm, Acacia frame) could break under stress during operation, potentially causing splinters or instability.	Trebuchet constructed with robust wood and secured joints. Prior to each experiment session, a visual inspection of the trebuchet for cracks, loose joints, or wear is conducted. Operation is stopped immediately if any structural weakness is detected.
Counterweight Hazard	A falling 1.00 kg counterweight could cause crush or impact injuries, especially to hands or feet if caught underneath.	Ensure clear space beneath the counterweight's drop path. Feet are kept clear of the counterweight's drop zone at all times during operation. Handle counterweight with care when setting up and resetting the trebuchet.
Pinch Points	Moving parts of the trebuchet, especially around the fulcrum and sling attachment, create pinch points that could trap fingers or clothing.	Avoid placing hands or loose clothing near moving parts during operation. Maintain awareness of pinch points and ensure safe distances are kept during launches and resets.
Eye Injury	Payload or wood splinters could potentially cause eye injury during launch or structural failure.	Safety glasses or goggles are worn by all individuals within the safety perimeter throughout the experiment.
Material Handling	Sharp edges or splinters from the wooden trebuchet components could cause cuts or puncture wounds during construction and handling.	Wear gloves during construction and when handling the trebuchet if necessary. Inspect wooden components for splinters and smooth down any sharp edges before operation. First aid kit is readily available.

Table 4: Risk assessment.

2 Analysis

2.1 Data Collection

2.1.1 Qualitative Data

Video recordings of launches confirmed visual trends. Shorter sling lengths (e.g., $L_s = 0.10$ m) resulted in earlier release, higher trajectories (larger θ), and shorter horizontal ranges (R). Conversely, increasing L_s (towards 0.40 m) led to later releases, lower angles (θ), and flatter trajectories. Visually, the maximum range appeared to occur within the tested L_s range, not at the longest length. The frame remained stable, with minimal airflow indoors. Minor launch smoothness variations (likely due to manual release) were observed, but no significant sling tangling occurred. The payload's first landing impact was consistently marked despite minor bouncing. Figure 5 illustrates the release angle measurement via Tracker software.

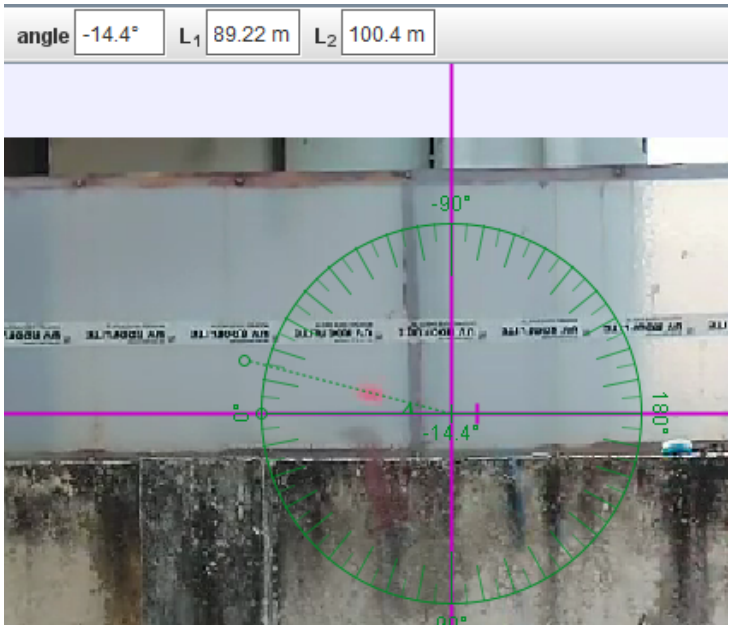

Figure 5: Sample Tracker screenshot showing trajectory analysis for $L_s = 0.20$ m, Trial 1. Release angle (θ) determined from the velocity vector tangent (red line) relative to horizontal (blue line) at release.

2.1.2 Quantitative Data

The following tables present the raw data collected for the horizontal range (R) and release angle (θ) for each of the five trials conducted at the seven different sling lengths (L_s). R was measured using a measuring tape and θ was determined using Tracker video analysis.

Sling Length (L_s) / m	Horizontal Range (R) / m				
	Trial 1	**Trial 2**	**Trial 3**	**Trial 4**	**Trial 5**
0.10	4.45	4.61	4.52	4.39	4.55
0.15	5.88	5.75	5.92	5.81	5.79
0.20	6.87	6.82	6.88	6.79	6.95
0.25	7.55	7.41	7.63	7.48	7.51
0.30	7.88	7.95	7.76	7.82	7.91
0.35	7.65	7.78	7.59	7.71	7.61
0.40	7.18	7.31	7.25	7.09	7.22

Table 5: Raw data for horizontal range (R) measured with a measuring tape.

Sling Length (L_s) / m	Release Angle (θ) / °				
	Trial 1	**Trial 2**	**Trial 3**	**Trial 4**	**Trial 5**
0.10	23.50	22.80	23.10	24.00	23.60
0.15	18.80	19.50	18.20	19.10	18.60
0.20	14.40	13.80	14.00	14.40	13.90
0.25	11.90	11.10	11.50	10.80	11.20
0.30	9.40	8.70	9.10	9.60	8.90
0.35	7.90	7.20	7.50	8.10	7.70
0.40	6.50	5.80	6.10	6.80	6.30

Table 6: Raw data for release angle (θ) determined using Tracker software.

2.2 Data Processing

All data processing is presented below, including formulas and sample calculations for the first condition of sling length ($L_s = 0.10$ m will be used for the sample, adjust if needed, but I'll use $L_s = 0.20$m as before for consistency). The processed data will facilitate graphical analysis of the relationship between sling length and the dependent variables.

1. **Calculating the average horizontal range (R_{avg}) for each sling length.** The average range is calculated by summing the range values from the five trials (R_1 to R_5) and dividing by the number of trials (5).

$$R_{avg} = \frac{R_1 + R_2 + R_3 + R_4 + R_5}{5}$$

Sample Calculation for $L_s = 0.20$ m: Using the raw data from Table 5:

$$R_{avg} = \frac{6.87 + 6.82 + 6.88 + 6.79 + 6.95}{5} = \frac{34.31}{5} = 6.862 \text{ m}$$

2. **Calculating the uncertainty propagation of the average horizontal range (ΔR_{avg}) using the half-range method.** The uncertainty representing the random error in the repeated measurements is estimated as half the difference between the maximum (R_{max}) and minimum (R_{min}) values recorded for each sling length.

$$\Delta R_{avg} = \frac{R_{max} - R_{min}}{2}$$

Sample Calculation for $L_s = 0.20$ m:

$$R_{max} = 6.95 \text{ m}, \quad R_{min} = 6.79 \text{ m}$$

$$\Delta R_{avg} = \frac{6.95 - 6.79}{2} = \frac{0.16}{2} = 0.080 \text{ m}$$

Therefore, for $L_s = 0.20$ m, $R_{avg} = 6.86 \pm 0.08$ m (rounding average to match uncertainty).

3. **Calculating the average release angle (θ_{avg}) for each sling length.** The average angle is calculated by summing the angle values from the five trials (θ_1 to θ_5) and dividing by the number of trials (5).

$$\theta_{avg} = \frac{\theta_1 + \theta_2 + \theta_3 + \theta_4 + \theta_5}{5}$$

Sample Calculation for $L_s = 0.20$ m: Using the raw data from Table 6:

$$\theta_{avg} = \frac{14.4 + 13.8 + 14.0 + 14.4 + 13.9}{5} = \frac{70.5}{5} = 14.10 \text{ }^\circ$$

4. **Calculating the uncertainty propagation of the average release angle ($\Delta\theta_{avg}$) using the half-range method.** The uncertainty is estimated as half the difference between the maximum (θ_{max}) and minimum (θ_{min}) values recorded for each sling length.

$$\Delta\theta_{avg} = \frac{\theta_{max} - \theta_{min}}{2}$$

Sample Calculation for $L_s = 0.20$ m:

$$\theta_{max} = 14.4 \text{ }^\circ, \quad \theta_{min} = 13.8 \text{ }^\circ$$

$$\Delta\theta_{avg} = \frac{14.4 - 13.8}{2} = \frac{0.6}{2} = 0.30 \text{ }^\circ$$

Therefore, for $L_s = 0.20$ m, $\theta_{avg} = 14.1 \pm 0.3$ ° (rounding average and uncertainty to one decimal place).

The processed results for all sling lengths are presented in Table 7.

Sling Length L_s / **m**	**Avg. Horiz. Range** $R_{avg} \pm \Delta R_{avg}$ / **m**	**Avg. Release Angle** $\theta_{avg} \pm \Delta\theta_{avg}$ / **°**
0.10	4.50	23.4 ± 0.6
0.15	5.83	18.8 ± 0.7
0.20	6.86	14.1 ± 0.3
0.25	7.52	11.3 ± 0.6
0.30	7.86	9.1 ± 0.5
0.35	7.67	7.7 ± 0.5
0.40	7.21	6.3 ± 0.5

Table 7: Processed data: Average horizontal range and average release angle with uncertainties calculated using the half-range method.

5. **Plotting the data.** Graphs of the average horizontal range (R_{avg}) versus sling length (L_s) and average release angle (θ_{avg}) versus sling length (L_s) were plotted using the processed data from Table 7. Error bars representing the uncertainty (ΔR_{avg} and $\Delta\theta_{avg}$) were included for each data point.

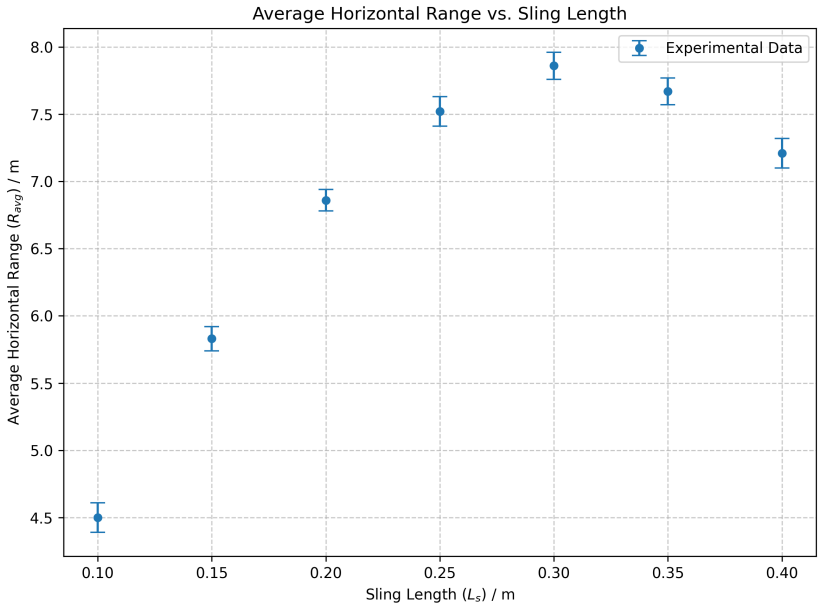

Figure 6: Graph of Average Horizontal Range (R_{avg}) vs Sling Length (L_s). Error bars represent the uncertainty ΔR_{avg} (half-range).

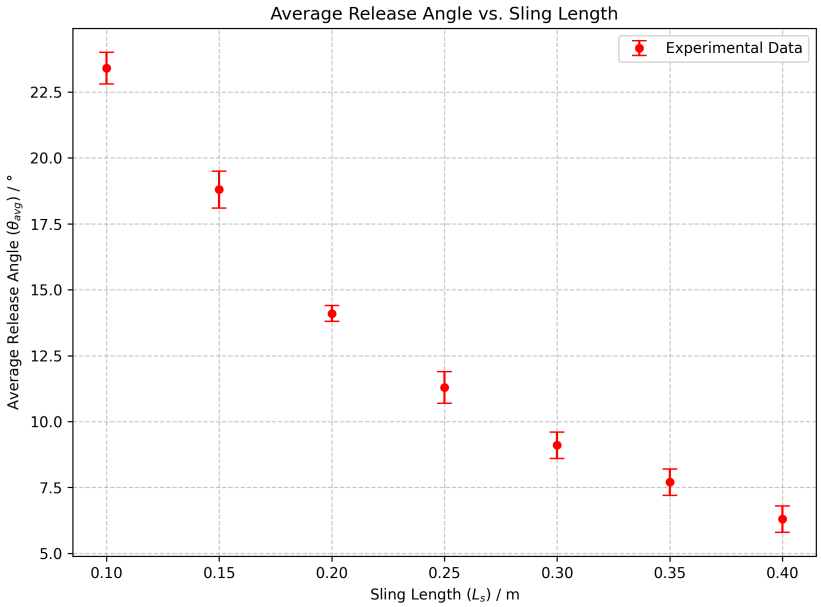

Figure 7: Graph of Average Release Angle (θ_{avg}) vs Sling Length (L_s). Error bars represent the uncertainty $\Delta\theta_{avg}$ (half-range).

3 Conclusion

This investigation examined how varying sling length (L_s) affects the horizontal range (R) and release angle (θ) of a model trebuchet, under controlled conditions (0.050 kg payload, 1.00 kg counterweight, 0.4133 m lever arm, 0.30 m drop height).

Experimental analysis revealed significant, non-linear relationships. Average horizontal range (R_{avg}) increased from 4.50 ± 0.11 m ($L_s = 0.10$ m) to a maximum of 7.86 ± 0.10 m at an optimal $L_s = 0.30$ m, before decreasing for longer L_s values (Figure 6). Concurrently, average release angle (θ_{avg}) decreased non-linearly from $23.4 \pm 0.6°$ ($L_s = 0.10$ m) to $6.3 \pm 0.5°$ ($L_s = 0.40$ m) as L_s increased (Figure 7).

These results strongly support the alternative hypothesis (H_1)—that L_s significantly correlates with R and θ, with an optimal L_s for maximizing range—allowing rejection of the null hypothesis (H_0).

The findings align with the theoretical range equation $R = \frac{k^2(L_a+L_s)^2 \sin(2\theta)}{g}$. The data suggests the increase in the $(L_a + L_s)^2$ term initially dominates, increasing range despite decreasing θ. Beyond the experimentally determined optimum $L_s = 0.30$ m, the reduction in the $\sin(2\theta)$ term becomes more significant, causing range to decrease. This optimum represents the configuration balancing these competing factors for maximum range.

Therefore, sling length is a critical parameter influencing this model trebuchet's range and release angle non-linearly. An optimal sling length of 0.30 m maximized the horizontal range under the specific experimental constraints.

4 Evaluation

4.1 Uncertainty

The uncertainties calculated for the average range (ΔR_{avg}) and average release angle ($\Delta\theta_{avg}$) reflect the random variations observed across the five trials for each sling length. As shown in Table 7, the range uncertainty (ΔR_{avg}) varied from a minimum of ± 0.08 m (at $L_s = 0.20$ m) to a maximum of ± 0.11 m (at $L_s = 0.10$ m and $L_s = 0.25$ m, $L_s = 0.40$ m). Similarly, the angle uncertainty ($\Delta\theta_{avg}$) ranged from $\pm 0.3°$ (at $L_s = 0.20$ m) to $\pm 0.7°$ (at $L_s = 0.15$ m). This variation in spread across different sling lengths is expected and likely stems from subtle inconsistencies in the manual release process, minor variations in sling behavior (e.g., minimal stretching or tangling not easily visible), and the inherent challenges in precisely marking the landing spot and determining the exact release frame in Tracker, which might be slightly more pronounced for certain launch trajectories. While these random errors introduce scatter, the calculated uncertainties are relatively small compared to the overall range achieved (e.g., ± 0.10 m uncertainty on a range of ≈ 7.8 m represents about 1.3

Beyond these quantifiable random errors, several potential systematic errors could have influenced the results.

- **Air Resistance:** Although minimized by conducting the experiment indoors, air resistance acting on the lightweight payload (0.050 kg) would systematically reduce the actual horizontal range (R) compared to the ideal trajectory assumed in the background theory. This effect would likely be more significant at higher launch velocities, potentially affecting launches near the optimal sling length more, and could slightly shift the observed optimal L_s compared to a vacuum condition.

- **Fulcrum Friction:** Energy losses due to friction at the trebuchet's pivot point would systematically decrease the energy transferred to the payload, resulting in a lower initial velocity (v_0) and consequently a shorter range (R) across all trials than predicted by ideal energy conservation.
- **Instrument Accuracy:** The measuring tape (± 0.005 m), ruler (± 0.001 m), and digital scale (± 0.001 kg) have inherent limitations. While small, these could introduce minor systematic offsets in the measured values of R, L_s, L_a, m_p, and m_c. The calibration within Tracker software using the arm length also carries uncertainty.
- **Camera Parallax and Angle Measurement:** If the camera was not perfectly perpendicular to the plane of motion, parallax errors could affect the angle measurements in Tracker. Furthermore, the software's precision in determining the tangent at release (estimated $\pm 0.5^\circ$) constitutes a potential systematic limitation on the accuracy of θ.
- **Assumption of $g = 9.81$ $\mathbf{m/s^2}$:** Local variations in gravitational acceleration are negligible for this scale of experiment.

In summary, random errors explain the data scatter (reflected in error bars), while systematic errors (e.g., air resistance, friction) likely resulted in measured ranges consistently below idealized theoretical predictions. Nevertheless, the clear observed trends—a peak range and decreasing release angle—allowed for valid conclusions regarding the L_s-R-θ relationship and the identification of an optimal sling length despite these uncertainties.

4.2 Comparison

Experimental results align qualitatively with the theoretical model $R = \frac{k^2(L_a+L_s)^2 \sin(2\theta)}{g}$. The observed non-linear, peaked relationship between average range and L_s (Figure 6) supports the model's competing factors: the $(L_a + L_s)^2$ term and the $\sin(2\theta)$ term. The data clearly identifies an optimal $L_s = 0.30$ m yielding the maximum range (7.86 ± 0.10 m).

Similarly, the monotonically decreasing trend of average release angle θ_{avg} with increasing L_s (Figure 7), from $23.4 \pm 0.6^\circ$ to $6.3 \pm 0.5^\circ$, corroborates literature [1, 2] and trebuchet mechanics: longer slings lead to later, shallower releases.

The optimal $L_s = 0.30$ m is shorter than the lever arm $L_a = 0.4133$ m. This deviation from some idealized models (suggesting $L_s \approx L_a$ [2]) is plausible, likely due to real-world factors like energy losses (friction, drag), release geometry, and sling dynamics, which are often simplified in theoretical treatments [2].

Further testing the model (Eq. 17) by calculating the proportionality factor k ($k = \sqrt{\frac{R_{avg} g}{(L_a+L_s)^2 \sin(2\theta_{avg})}}$) using processed data yields reasonably consistent values across different L_s. This lends additional support to the derived model, though variations likely reflect model simplifications (neglected losses/flex) and experimental uncertainties.

In summary, the data strongly supports the established physics relating L_s, R, and θ, and quantitatively identifies an optimal L_s for this specific trebuchet.

4.3 Weaknesses and Limitations

The investigation faced several weaknesses inherent in the experimental setup and methodology, which are summarized in Table 8. These limitations primarily contribute to the

uncertainties discussed previously and may explain deviations from idealized theoretical predictions.

Table 8: Weaknesses and limitations of the investigation.

Source of Error / Limitation	**Impact on the Results**	**Suggested Improvement**
Sling release inconsistency	Variations in release timing/smoothness due to manual release or slight pouch behavior differences could contribute significantly to the observed scatter in R and θ (seen in ΔR_{avg}, $\Delta\theta_{avg}$), reducing precision and potentially obscuring the true functional relationship.	Implement a standardized mechanical release mechanism (e.g., a trigger holding and releasing the sling pouch ring) for more consistent release timing and angle.
Teakwood arm flexibility	The Teakwood arm likely flexed under load, especially during acceleration. This absorbs energy that would otherwise go to the projectile, reducing v_0 and R. The amount of flex might vary slightly between trials or with L_s, adding uncontrolled variability.	Use a stiffer material for the arm (e.g., laminated wood, metal T-slot extrusion, carbon fiber tube) or reinforce the existing arm with bracing to minimize flex.
Handmade alignment errors	Minor misalignments in the frame construction, fulcrum pivot, or arm straightness (inherent in hand-built wooden structures) could cause the launch plane to deviate slightly from vertical or introduce sideways motion, affecting the measured horizontal range R and potentially the release dynamics θ.	Use precision tools (e.g., jigs, laser level, machinist square) during construction. Ensure the fulcrum axle is perfectly perpendicular to the arm and frame supports.
Video analysis limitations (Tracker)	Camera frame rate (e.g., 30 fps) limits the temporal resolution for pinpointing the exact moment of release. Parallax error if the camera wasn't perfectly perpendicular. Difficulty tracking a small, fast object accurately. These contribute to the uncertainty in θ ($\pm 0.5^\circ$ or more).	Use a high-speed camera (e.g., 120 fps or higher) for better temporal resolution. Ensure precise camera alignment. Use high-contrast markers on the payload if possible.

Continued on next page

Table 8 – continued from previous page

Source of Error / Limitation	Impact on the Results	Suggested Improvement
Air Drag	Although conducted indoors, air resistance acting on the 0.050 kg payload would reduce its actual range compared to the vacuum trajectory assumed in Eq. 1. This effect increases with velocity, potentially affecting longer-L_s launches more significantly, thus slightly distorting the shape of the R vs L_s curve.	Use a denser, more aerodynamic payload if possible (while keeping mass constant). Develop a theoretical model incorporating drag (more complex) or acknowledge this as a systematic deviation.
Fulcrum Friction	Energy loss due to friction at the pivot point reduces the energy transferred to the payload, lowering v_0 and R. Assumed small, but likely present and potentially variable.	Use low-friction bearings (e.g., ball bearings) for the fulcrum instead of a simple axle, and ensure proper lubrication.
Sling Elasticity	The wool cord likely stretched under tension during the swing, storing elastic potential energy. Its release might not be perfectly timed or consistent, adding variability to v_0 and θ.	Use a less elastic material for the sling cord (e.g., braided nylon, Spectra line) while maintaining flexibility for release.

Addressing these weaknesses, particularly improving release consistency and using a stiffer arm, would likely reduce the random scatter and bring experimental results closer to theoretical predictions based on energy conservation.

4.4 Strengths

Despite the limitations, the investigation possessed several strengths that contribute to the validity of its findings, as outlined in Table 9. These factors ensured that the primary relationship under investigation could be clearly observed.

Strength	Significance
Controlled variables	Key parameters (L_a, m_c, m_p, h, fulcrum position) were carefully measured and kept constant within measurement uncertainty, successfully isolating L_s as the primary independent variable affecting R and θ. This allowed for observation of clear trends despite inherent variability.
Video analysis (Tracker)	Using Tracker software allowed for quantitative measurement of the release angle (θ), which is difficult to measure accurately otherwise. It provided objective data on the trajectory dynamics, enhancing the reliability of angle measurements despite camera limitations.
Multiple trials and uncertainty analysis	Conducting five trials per sling length allowed for the calculation of average values and an estimation of random uncertainty (ΔR_{avg}, $\Delta\theta_{avg}$). This provides a measure of data reliability and allows for more robust conclusions about the observed trends and the significance of the optimal point.
Systematic investigation	Varying the sling length over a wide range (0.10 m to 0.40 m) in regular increments provided sufficient data points to clearly map the non-linear relationship for both range and angle, allowing for the identification of the peak range.
Preliminary trials	Conducting preliminary trials helped refine the methodology (sling pouch choice, drop height confirmation) and identify potential issues (tangling, frame clearance), leading to smoother data collection and more reliable results in the main experiment by minimizing easily avoidable errors.
Risk Assessment and Safety	A thorough risk assessment was conducted, and appropriate safety measures (safety glasses, clear area) were implemented, ensuring the experiment was performed safely without incident.

Table 9: Strengths of the investigation.

The careful control of variables and the use of video analysis were particularly crucial in obtaining meaningful data from a complex mechanical system like a trebuchet.

References

[1] Trebuchet Physics. (n.d.). Real World Physics Problems. https://www.real-world-physics-problems.com/trebuchet-physics.html

[2] Siano, Donald B. "Trebuchet Mechanics." The Algorithmic Beauty of the Trebuchet (2001). https://www.gomakos.org/ourpages/auto/2016/9/20/33121317/trebmath35.pdf